

NASA Technical Memorandum 100194

Ground-Based Plasma Contactor Characterization

Michael J. Patterson
Lewis Research Center
Cleveland, Ohio

and

Randall S. Aadland
University of Washington
Seattle, Washington

Prepared for the
Second International Conference on Tethers in Space
cosponsored by the ESA, AIAA, and AAS
Venice, Italy, October 6-8, 1987



(NASA-TM-100194) GROUND-BASED PLASMA
CONTACTOR CHARACTERIZATION (NASA) 17 p
Avail: NTIS HC AC2/MF A01 CSCL 20I

N87-28423

Unclas
G3/75 0094203

GROUND-BASED PLASMA CONTACTOR CHARACTERIZATION

Michael J. Patterson*
NASA Lewis Research Center
Cleveland, Ohio 44135

Randall S. Aadland**
University of Washington
Seattle, Washington 98105

Abstract

This paper presents recent NASA Lewis Research Center (LeRC) plasma contactor experimental results, as well as a description of the plasma contactor test facility. The operation of a 24cm diameter plasma source with hollow cathode was investigated in the "ignited-mode" regime of electron current collection from 0.1 to 7.0 A. These results are compared to those obtained with a 12cm plasma source. Full two-dimensional plasma potential profiles were constructed from emissive probe traces of the contactor plume. The experimentally measured dimensions of the plume sheaths were then compared to those theoretically predicted using a model of a spherical double sheath. Results are consistent for currents up to approximately 1.0 A. For currents above 1.0 A, substantial deviations from theory occur. These deviations are due to sheath asphericity, and possibly volume ionization in the double-sheath region.

Nomenclature

A	ampere
J_B	bias current ($= J_0$), (A)
J_{CD}	contactor discharge current, (A)
J_0	collected electron current, (A)
J_{SD}	simulator discharge current, (A)
J_{SE}	simulator emission current, (A)
R_i	radius of inner sheath, (cm)
R_o	radius of outer sheath, (cm)
sccm	standard cubic centimeters per minute
SPS	space plasma simulator
V	volt
V_B	bias voltage, (V)
V_{CD}	contactor discharge voltage, (V)
V_P	ambient plasma potential, (V)
V_{SD}	simulator discharge voltage, (V)

Introduction

A variety of propulsive and power generation applications have been identified for space tethers, involving electrodynamic interactions of a conductive wire with planetary magnetic fields.^{1,2,3} These applications are critically dependent on the development

and demonstration of plasma contactor technology.⁴ Recent research efforts with hollow cathode-based plasma contactors at NASA LeRC indicate that multi-ampere level electron currents, sufficient for electrodynamic tether operation, can be exchanged between these devices and a dilute plasma via operation in an "ignited-mode."^{4,5} These results have been independently verified in experiments conducted at current levels one-to-two orders of magnitude below those observed in the NASA LeRC experiments.⁶ In this mode of operation, significant volume ionization occurs in the plume due to the backstreaming electron current. For contactors with large effective anode area, virtually identical current-voltage characteristics are observed with or without discharge power to the contactor. This suggests that ionization due to collected electron current is at least as large as ionization due to contactor cathode electrons. For reasons of efficiency, therefore, operation in the "ignited-mode" is preferred.

These experiments have demonstrated the feasibility of plasma contactor bipolar operation. However, there is not yet sufficient understanding of the plasma contacting process observed in the laboratory to reliably predict contactor performance in space-based experiments. Theoretical predictions of a simple model of a space-charge-limited double-sheath⁷ have shown good agreement with experimental data for the range of electron current collection investigated (up to several hundred milliamperes).⁶ However a recent analysis suggests that these results may be substantially impacted by the size of the space simulation chamber.⁸

Consequently, a program was initiated at NASA LeRC (in a facility with 50 times the volume of the chamber in ref. 6) to:

- 1.) verify the formation of a space-charge-limited double-sheath; and
- 2.) determine the extent of validity of the double-sheath model over a wide range of electron collection current (0.1 to >5.0 A).

*Aerospace Engineer, Member AIAA.
**Graduate Student.

Plasma Contactor Test Facility

The facility used in the plasma contactor experiments is located in the Electric Propulsion Laboratory of NASA LeRC. The Electric Propulsion Laboratory was designed for testing plasma thrusters, spacecraft, and other hardware in a simulated space environment. The facility consists of a large vacuum tank of dimensions 4.6m diameter by 19.2m long, a central control room to remotely conduct the experiment, a clean room, and a shop area to provide electrical, electronic, and mechanical test support. The experiment power supplies, the tank pumping systems, a sheet metal shop, and storage areas are all located on a lower level of the laboratory. A thorough description of this laboratory (which includes several other large vacuum tanks) can be found in ref.9.

The vacuum tank has a pumping train consisting of twenty 81cm diffusion pumps, four blowers, and four roughing pumps. The base pressure (without flow) is approximately 9×10^{-7} torr with a maximum pressure of 7×10^{-6} torr at the highest total flowrate of xenon (20.6 sccm) used in these experiments. The tank is fully automated for around-the-clock unattended operation. At present, there are two 0.9m access ports with gate valves - one located on the tank endcap at centerline, and a second located at approximately the half-way point of the chamber length. The plasma contactor, and one of the space plasma simulators (electron source) are located on individual experiment carts which can be rolled into and out of these ports. After cart installation, the port is evacuated and the gate valve to the main chamber is opened. The experiment can then be extended into the tank by the use of a drawer-slide and push-pull assembly. By reversing this sequence, rapid access to test hardware can be accomplished without bringing the entire tank to atmosphere. There are a number of other smaller ports, as well as electrical penetrations and windows located on the tank.

Hardware has been hard-mounted into the large vacuum tank to support an enhanced diagnostics capability of the plasma contactor environment. These include four Bayard-Alpert type ionization gauges and a movable array of five Langmuir probes, all of which are mounted such that they are on the vertical centerline of the tank. Figure 1 shows the relative location of this hardware.

In addition to the space plasma simulator (SPS) on the experiment cart, three other SPS units are also mounted in the tank. Each SPS unit can be operated independently or in any combination to provide the ambient plasma from which the

contactor draws current. These devices are also mounted such that they are on the vertical centerline of the tank. The separation of the plasma contactor (when fully extended into the tank endcap port) from SPS-1 & 4 is 8.60m, and 3.54m from SPS-2 & 3.

The plasma contactor cart is equipped with push-pull assemblies which permit emissive or Langmuir probe motion from the plane of the plasma contactor out to an axial distance of 125cm along the device centerline. Additionally, these assemblies can be rotated allowing measurements at various radii from 0 to 50cm. This set-up can also accommodate the use of other diagnostics, including an electron energy analyser and an ionization gauge to map the contactor environment in both the axial and radial positions.

Plasma Contactor Characterization

This section presents the experimental apparatus and procedure employed in characterization of plasma contactor operation. A synopsis of the performance of a 24cm NASA LeRC contactor and a 12cm CSU contactor, both tested at the LeRC facility, is presented in the form of current-voltage characteristics. Correlations of experimentally measured-to-theoretically predicted (using a spherical double sheath model) profiles of the contactor plumes are also presented.

Experimental Apparatus and Procedure

In order to investigate the behavior of a plasma contactor in the electron current collection mode, a test configuration like that shown in Fig. 2 was constructed. In general, the test scenario consists of a plasma contactor (located at the endcap port) and the space plasma simulators (SPS-1,2,3, & 4), all of which are hollow cathode devices. In these experiments, the SPS units are electrically tied to tank ground through cathode common. The plasma contactor anode is electrically tied to the positive side of bias supply whose opposite side is then tied to tank ground. The plasma contactor can then be biased positive with respect to both the tank and the plasma generated by the simulators so that the contactor can collect electron current from the background plasma. The system allows for flexibility to rapidly reconfigure the circuit to permit biasing of the contactor for electron current emission studies, or to electrically isolate the contactor-simulator system from tank ground.

The NASA LeRC 24cm plasma contactor used during this investigation is shown in Fig. 3. The contactor is essentially a hollow cathode assembly with the attachment of a second, or auxiliary, anode constructed of 0.8mm thick stainless steel. The 24cm dimension refers to the diameter of the auxiliary anode which collects of electron current coming from the ambient plasma when biased. The auxiliary anode is concentric with a sustaining anode constructed of tantalum. The hollow cathode assembly consists of a 0.64cm diameter tantalum tube with an electron-beam welded thoriated tungsten orifice plate on one end. The orifice plate has a centered 2.0mm hole drilled through it. A porous tungsten insert impregnated with low work function material is located inside the hollow cathode to serve as a source of electrons. This device has an ion production capacity of approximately 18mA (as measured by biasing the contactor with respect to facility ground and measuring the ion saturation current to the tank walls), at a maximum power of 89 watts and flowrate of 13.7sccm. Reference is made to data obtained with a CSU plasma contactor as well. The CSU device is similar to the LeRC contactor described above, except for the size of the auxiliary anode (12cm diameter), and the type of hollow cathode insert (rolled tantalum foil coated with barium carbonate). A more thorough description of this contactor can be found in ref. 6.

The four SPS units used in these experiments are each identical to the hollow cathode assembly used in the 24cm plasma contactor. These units are oriented such that the cathode length runs parallel to the tank length, with the orifice directed toward the endcap port where the plasma contactor is mounted. Figure 4 shows a cross-section of an SPS unit. The standard operating condition for SPS-1 was 6.85sccm xenon at a discharge current (J_{SD}) of 3.5 A. The standard operation condition for SPS-2,3, & 4 were also 6.85sccm xenon, at a J_{SD} of 3.0 A. These conditions were fixed for the duration of the testing.

For the experiments described herein, the electron collection current capabilities of the plasma contactors were investigated as a function of bias voltage and contactor operating condition (expellant flowrate). The impact of the relative location of the SPS unit to the plasma contactor was also investigated by switching from SPS-1 through SPS-4 during operation. During electron current collection, emissive probe traces were made to characterize the contactor plume plasma potential profiles both in the axial and radial dimensions, in the manner previously described. The construction of the emissive probe is similar to that described in ref. 10. At each operating condition, V_{CD} , J_{CD} , V_B ,

J_B , V_{SD} , J_{SD} , and J_{SE} were measured using metering, as shown schematically in Fig. 2.

Plasma Contactor Performance

The results of the plasma contactor characterization can be divided into three separate experiments:

- 1.) Comparison of NASA LeRC 24cm contactor performance to CSU 12cm contactor;
- 2.) Impact of operating condition on performance of 24cm contactor; and
- 3.) Impact of simulator location on 24cm contactor performance.

Current-voltage characteristics, and double sheath model correlations are provided for each of these experiments.

A comparison of the current-voltage characteristic of the LeRC 24cm contactor and CSU 12cm contactor (in the electron current collection mode) is shown in Fig. 5. Plotted are the values of collected electron current (J_0) as a function of the bias voltage minus the ambient plasma potential ($V_B - V_P$). The value of V_P used is the ambient plasma potential as measured 125cm downstream of the plasma contactor. As indicated, for equivalent values of xenon flowrate (13.7sccm) and voltage, the level of collected electron current from SPS-1 to the 24cm contactor is more than an order-of-magnitude greater than that measured for the 12cm contactor. The voltages at which current began to be drawn to the contactor (4 V vs. 65 V), and the voltages at which operation transitioned into an "ignited-mode" (30 V vs. 110 V) are also substantially different. The ignited-mode is identified by a positive slope change in the V-I characteristic, accompanied by the appearance of a visible plume within which expellant excitation occurs. Although the use of dissimilar insert types precluded operation of the two contactors at identical power levels (24cm - 88.9 watts discharge power and zero watts heater power vs. 12cm - 8.80 watts discharge power at 68 watts heater power), this data would suggest an anode-area dependency of current collection.

For all test conditions in an ignited-mode, a double-sheath was observed in the contactor plume. Figure 6 shows an idealized plasma potential profile of the double-sheath including the locations of R_i and R_o . Figure 7 presents the correlation of the experimentally measured ratios of the inner to outer sheath radii (R_i/R_o) verses the radius ratios theoretically predicted using the model of a space-charge-limited spherical double-sheath. As indicated, the data for the CSU 12cm contactor shows good agreement. Results obtained for the LeRC

24cm contactor however diverge significantly from correlation, for electron current collection above 2.0 A. These data correspond to the rapid collapse of the inner sheath from a radius of 51.5cm down to approximately 12cm. This occurred at the onset of the "ignited-mode" of expellant excitation and presumably volume ionization due to streaming electron current.

It is of interest to note that the exterior sheath radii for both devices decrease in magnitude with increasing electron collection current. R_0 changed from 49.4cm to 31.2cm for collected currents from 0.11 to 1.92 A for the CSU device. For the LeRC contactor, R_0 decreased from 102.9cm to 66.5cm for collected currents from .095 to 2.50 A. Results from ref. 11 have shown that the location of the outer sheath boundary is defined such that the boundary surface area is equal to the collected electron current divided by the ambient plasma random current density. Consequently, these increases in collected electron current with decreasing collection sheath radii would correspond to increased ambient plasma thermal currents by factors of 10.5 and 63.1 for the CSU and LeRC contactor data respectively. This must be confirmed however by measurements of electron temperature and density in the ambient plasma.

Results obtained with the LeRC 24cm contactor at two different xenon expellant flowrates are shown in Figures 8 and 9. At the lower flowrate of 6.85sccm (facility pressure of 1.6×10^{-6} torr) the contactor did not transition into an ignited-mode operation. As indicated in Fig. 9, good correlation to the double-sheath model is achieved at this operating condition. However at the higher contactor flowrate (facility pressure of 2.5×10^{-6} torr) the results diverge significantly from those theoretically predicted, as previously discussed.

Contactor performance for current collection from each of the four SPS units is illustrated in Figs. 10, 11, and 12. Figure 10 shows that the contactor current-voltage characteristic is essentially independent of the relative location of the simulator. Figure 11 shows the model correlation for this data. It is not presently understood why the experimentally measured values of J_0 and $V_P - V_p$ predict values of radius ratio only in the range of 0.85-0.90. The percentage error of experimental-to-theoretical radius ratios are plotted as a function of collected electron current in Fig. 12. The deviation from perfect correlation increases for increasing values of collected electron current. However, the degree of deviation appears to be a function of the relative location of the SPS unit from the contactor. The

measured deviations for SPS-1 and SPS-4 current coupling, both of which are located 8.6m from the contactor, are comparable and in excess of 75% from perfect correlation for currents above 1.0 A. Contactor current coupling to SPS-2 and SPS-3 units, located closer to the plasma contactor (3.54m) show smaller deviations from perfect correlation.

Figures 7, 9, and 11 show that the deviations from the space-charge-limited spherical double-sheath condition are negative. That is, the measured ratio of R_i/R_0 is lower than that predicted by theory for a given value of collected current and voltage drop. The model predicts that the inner sheath radii should be larger than those measured. If volume ionization in the double-sheath is negligible, the disagreement between theory and experimental results should be explainable in terms of double-sheath development over a spherical surface less than four pi steradians in solid angle. However, calculating theoretical R_i/R_0 assuming less than a four pi solid angle further decreases the correlation of the data in Figures 7, 9, and 11 from the perfect fit line.

Figures 13-15 present two-dimensional surface and equipotential contour maps of the plasma potential plume of the 24cm contactor for an electron collection current of 0.23 A from SPS-1. At this operating condition, there was a perfect correlation of experimental to theoretical radius ratios of 0.77 (see Fig. 9). This corresponds to an inner radius of 47.5cm and an outer radius of 61.8cm, as implied by the potential profile in Fig. 14. The equipotential lines of Fig. 15 at these locations of R_i and R_0 indicate spherical sheath geometries.

At an electron current collection of 2.50 A from SPS-1, the deviation of experimental to theoretical radius ratios was -78.5%. Figures 16-18 present the surface and equipotential contour maps for this operating condition. The measured inner and outer sheath radii were 12.7cm and 66.5cm respectively (see Fig. 17). At these sheath locations, the equipotential lines in Fig. 18 suggest highly aspherical boundary conditions.

Figures 19 and 20 present contours of the plasma plume for electron collection currents from SPS-3 of 2.50 A and 5.90 A respectively. It is of interest that both conditions are at approximately -52% correlation of experimental to theoretical radius ratio, and are also observed to have comparable potential contour maps. At 2.50 A the inner radius is measured to be 20.6cm, while the 5.90 A condition has an inner radius of 15.9cm. Both conditions could be characterized as having aspherical (ellipsoidal) sheath formation.

Conclusion

Plasma contactor experiments conducted at the NASA LeRC plasma contactor test facility have verified the formation of a double-sheath during the electron current collection mode of plasma contactor operation.

Comparison of the performance of two contactors indicates that the level of electron current collection is influenced by the effective anode area of the contactor.

Theoretical predictions of the sheath radius ratios were obtained from a simple model of a space-charge-limited double-sheath. These predictions were compared to experimentally measured radius ratios obtained from emissive probe data. Good agreement was observed for electron current collection up to 1.0 A. Above this value, substantial deviations from theory occurred. This is apparently due to sheath asphericity, and possibly volume ionization in the double-sheath region.

Future experimental activities will include addressing issues of facility interactions, identifying the criteria which define R_i , and determining the mechanisms which influence the sheath geometry.

References

1. Bekey, I., "Tethers Open New Space Options," Astronautics and Aeronautics Volume 21, Number 4, April 1983, pp. 22-40.
2. Proceedings, Tether Applications In Space Program Review, General Research Corporation, McLean, Virginia, July 17-18, 1985.
3. Carroll, J. A., "Tether Applications In Space Transportation," Acta Astronautica, Volume 14, Number 4, April 1986, pp. 165-174.
4. Patterson, M.J., and Wilbur, P.J., "Plasma Contactors for Electrodynamic Tether," AAS Paper 86-226, September, 1986. (also published as NASA TM-88850.)
5. Patterson, M.J., and Wilbur, P.J., "Plasma Contactors for Electrodynamic Tethers," AIAA Aerospace AMERICA, pp.32-34, February, 1987.
6. Wilbur, P.J., and Williams, J., "An Experimental Investigation of the Plasma Contacting Process," AIAA Paper 87-0571, January, 1987.

7. Wei, R., and Wilbur, P.J., "Space-Charge-Limited Current Flow in a Spherical Double Sheath," J. Appl. Phys. 60(7), pp. 2280-2284, 1 October, 1986.
8. Katz, I., Davis, V.A., and Parks, D., "On The Need for Space Tests of Plasma Contactors as Electron Collectors," Second International Conference on Tethers in Space, Venice, Italy, October 6-8, 1987.
9. Finke, R.C., Holmes, A.D., and Keller, T.A., "Space Environment Facility For Electric Propulsion Systems Research," NASA TN D-2774, MAY, 1965.
10. Aston, G., "Ion Extraction from a Plasma," NASA CR-1159 849, pp. 12-19 June, 1980.
11. Williams, J.D., and Wilbur, P.J., "Experimental Validation of a Phenomenological Model of the Plasma Contacting Process," Second International Conference on Tethers in Space, Venice, Italy, October 6-8, 1987.

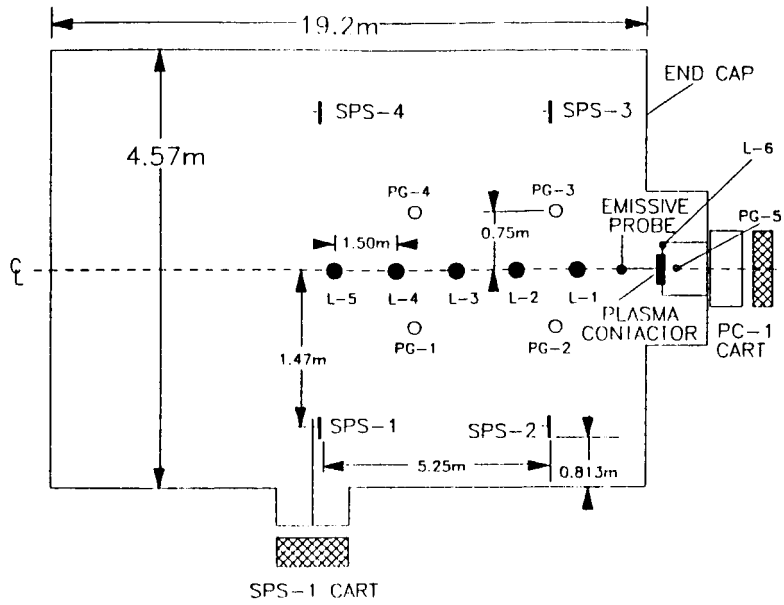


Fig. 1 Mechanical schematic of plasma contactor test facility. (SPS - space plasma simulator, PG - pressure gauge, L - Langmuir probe)

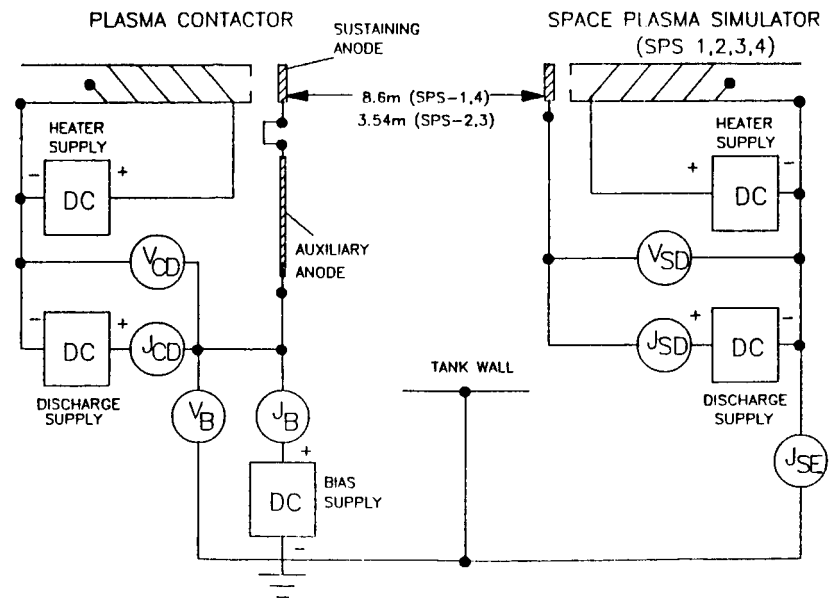


Fig. 2 Electrical schematic.

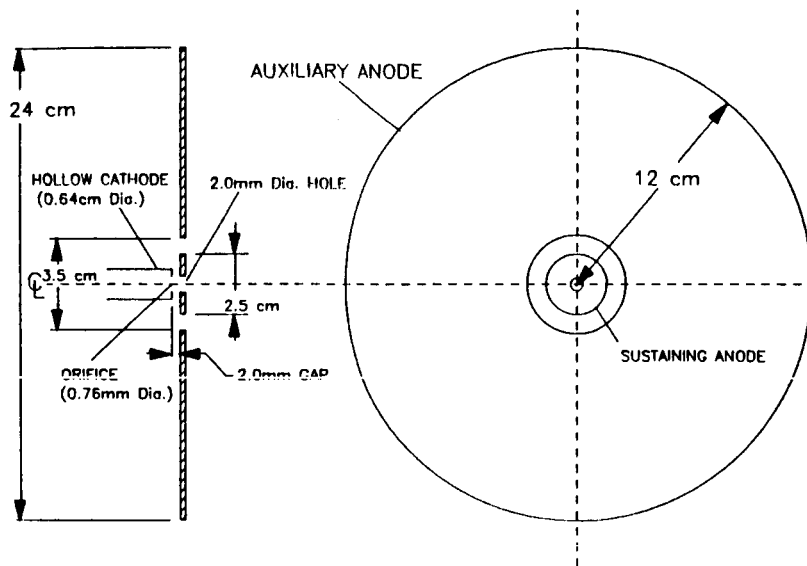


Fig. 3 NASA LeRC 24cm plasma contactor.

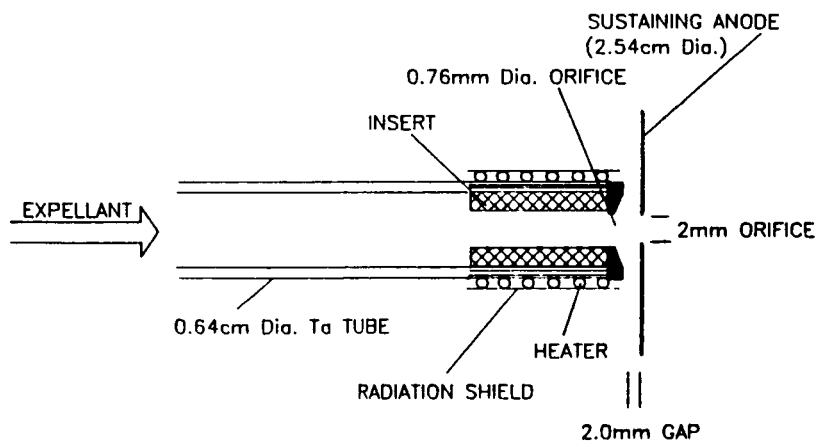


Fig. 4 Space plasma simulator (SPS).

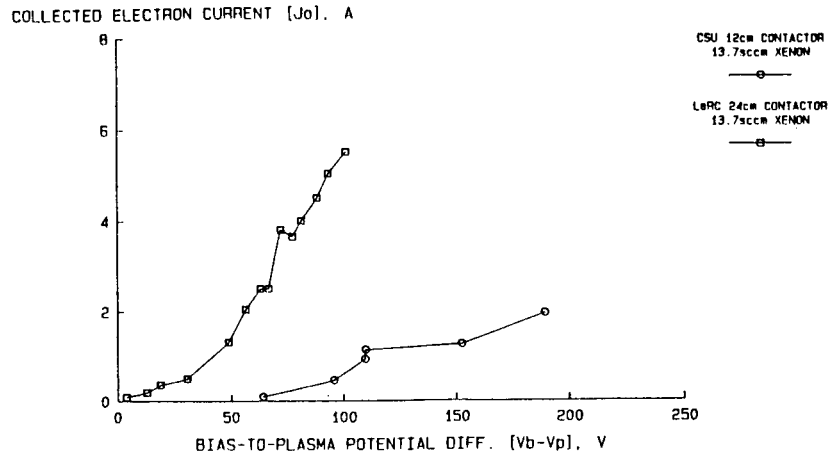


Fig. 5 Comparison of 24cm and 12cm contactor current-voltage characteristics.

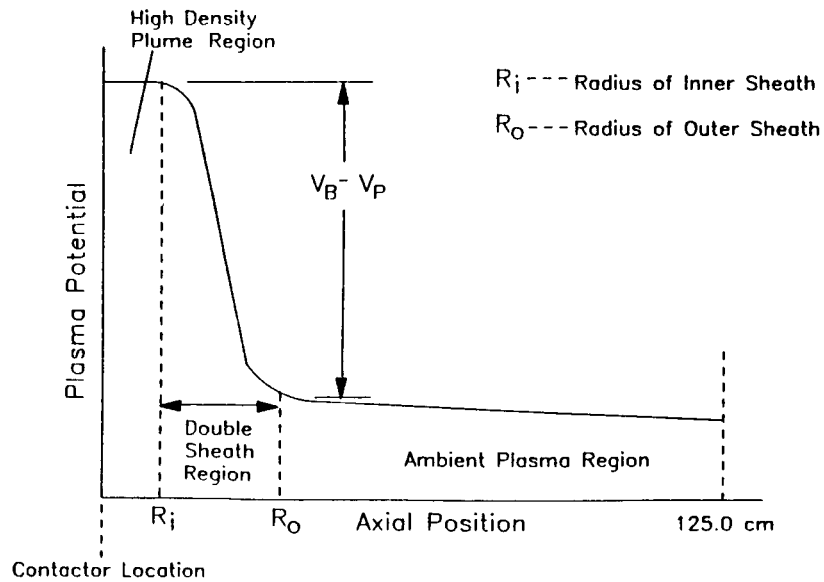


Fig. 6 Idealized double-sheath plasma potential profile.

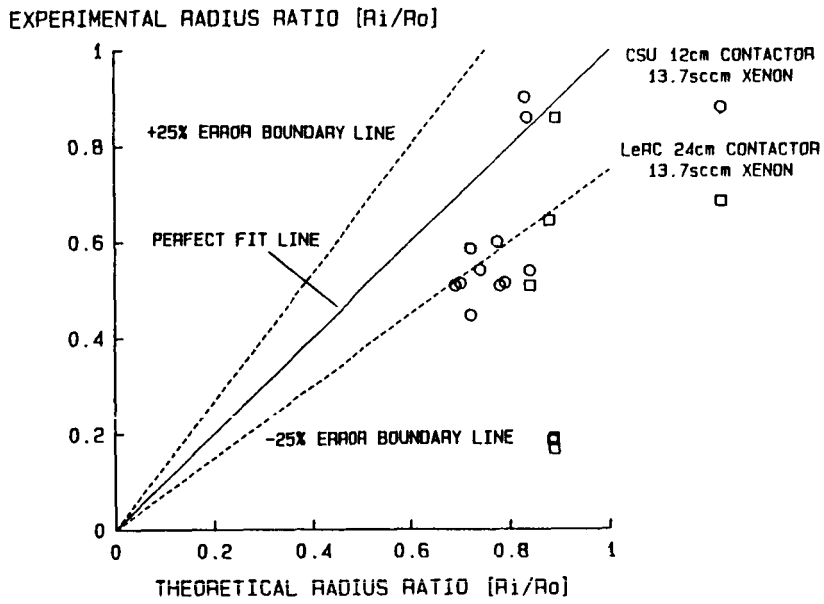


Fig. 7 Radius ratio comparison for 12cm and 24cm contactors. Current collection from SPS-1.

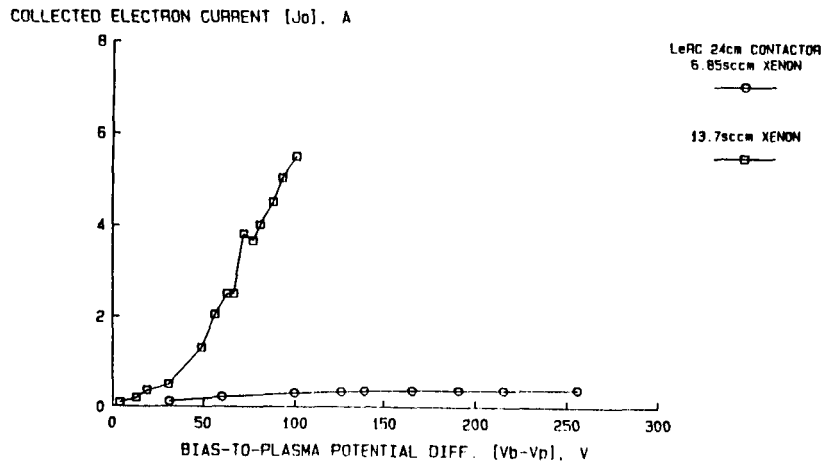


Fig. 8 Comparison of 24cm contactor current-voltage characteristics at two flowrates. Current collection from SPS-1.

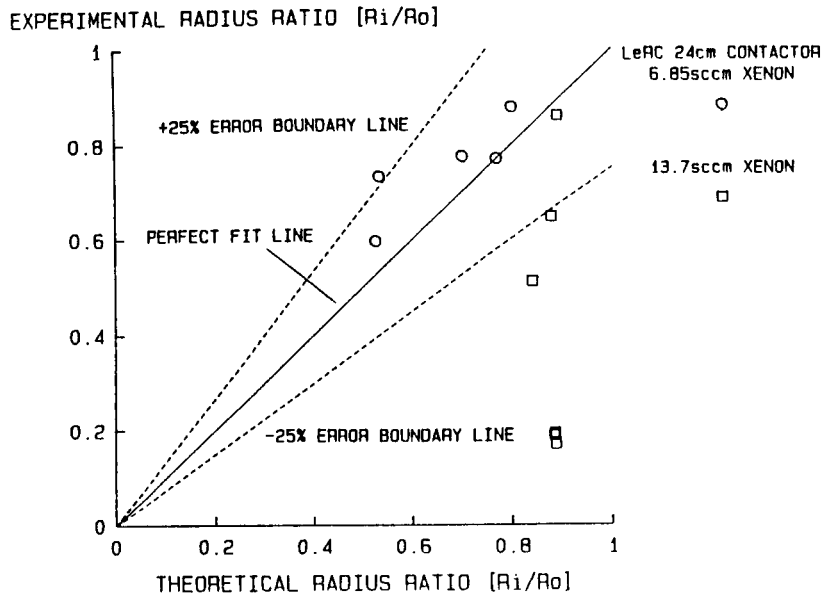


Fig. 9 Radius ratio comparison for 24cm contactor at two flowrates. Current collection from SPS-1.

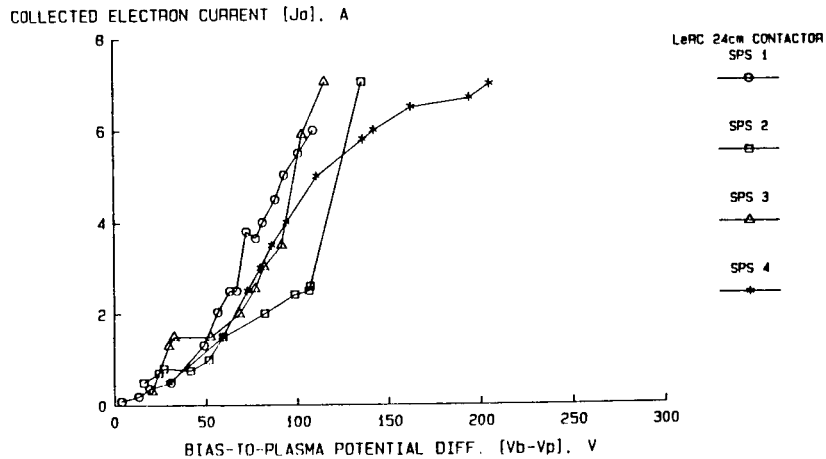


Fig. 10 Comparison of 24cm contactor current-voltage characteristics for different SPS units. Contactor flowrate 13.7sccm xenon.

LeRC 24cm CONTACTOR 6.85sccm XENON $J_0=0.23$ A

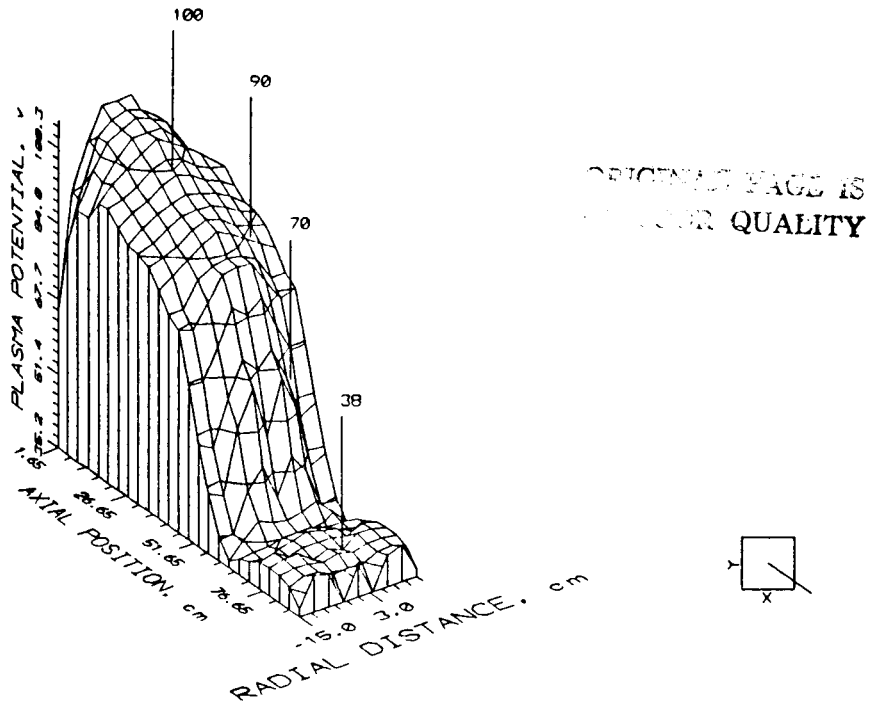


Fig. 13 Surface contour map of contactor plume for 0.23 A current collection from SPS-1.

LeRC 24cm CONTACTOR 6.85sccm XENON $J_0=0.23$ A

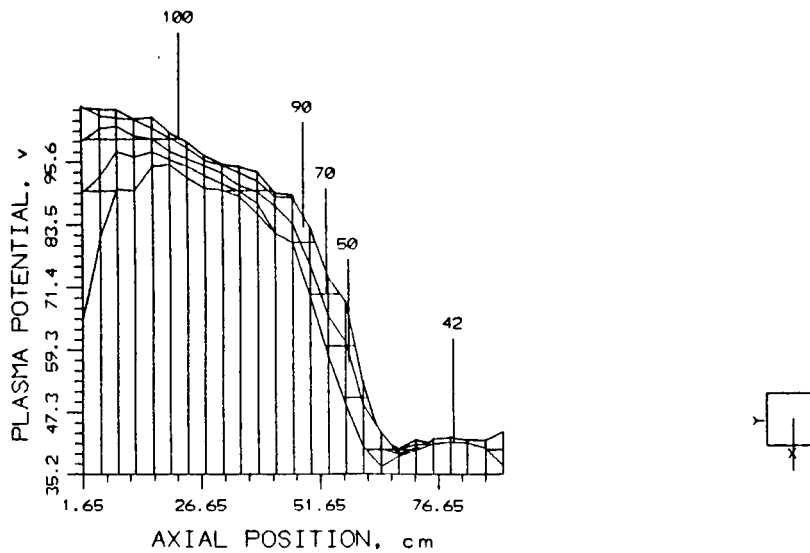


Fig. 14 Plasma potential profile of contactor plume for 0.23 A current collection from SPS-1.

ORIGINAL PAGE IS
OF POOR QUALITY

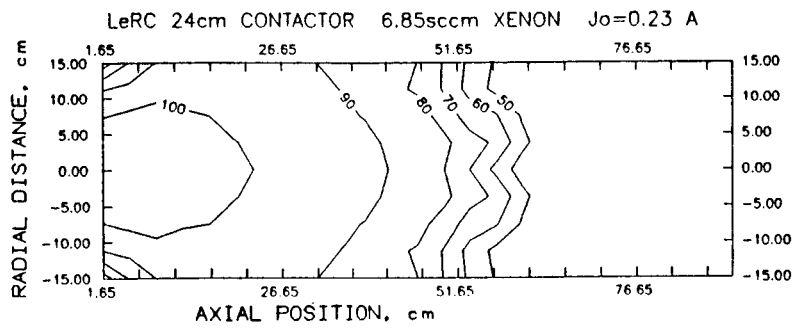


Fig. 15 Equipotential contour plot of contactor plume for 0.23 A current collection from SPS-1.

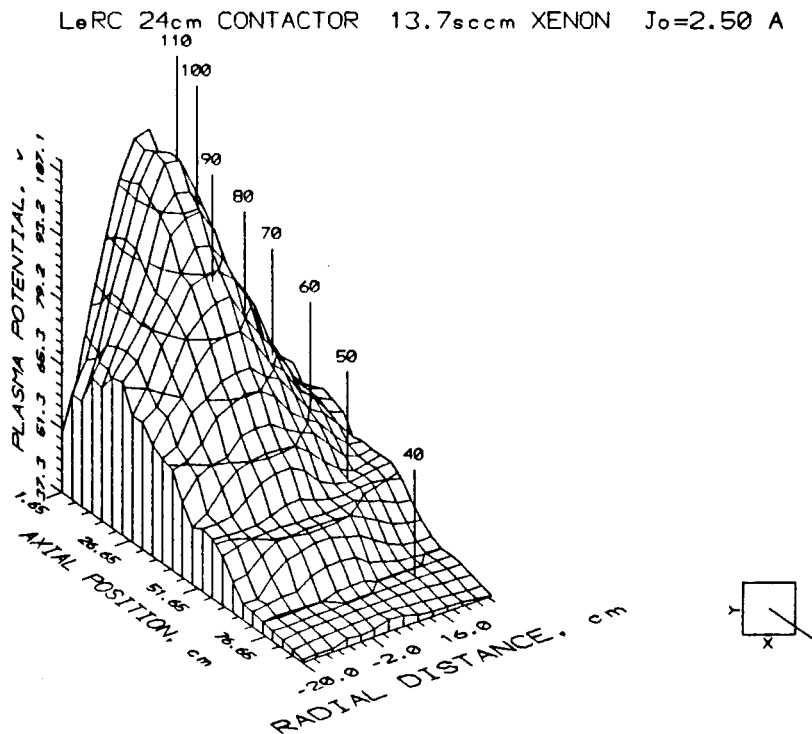


Fig. 16 Surface contour map of contactor plume for 2.50 A current collection from SPS-1.

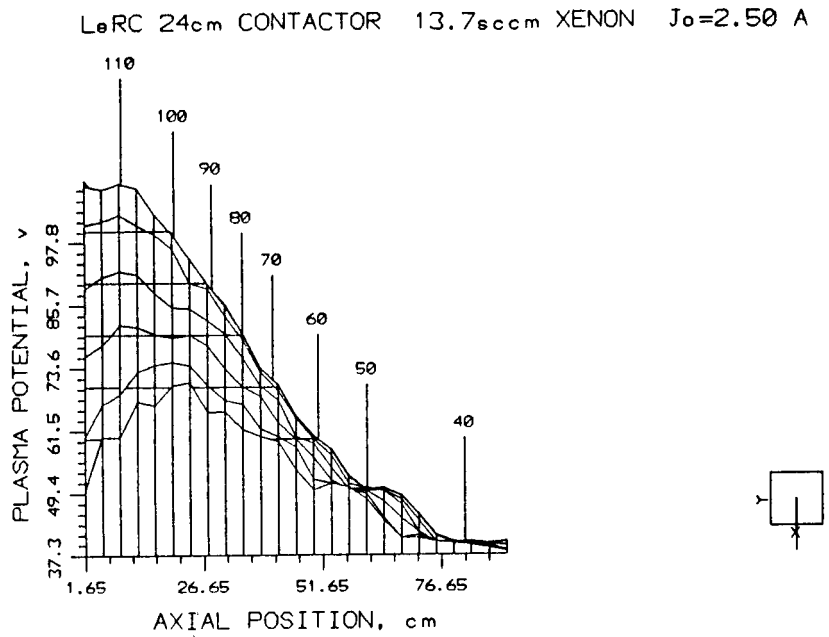


Fig. 17 Plasma potential profile of contactor plume for 2.50 A current collection from SPS-1.

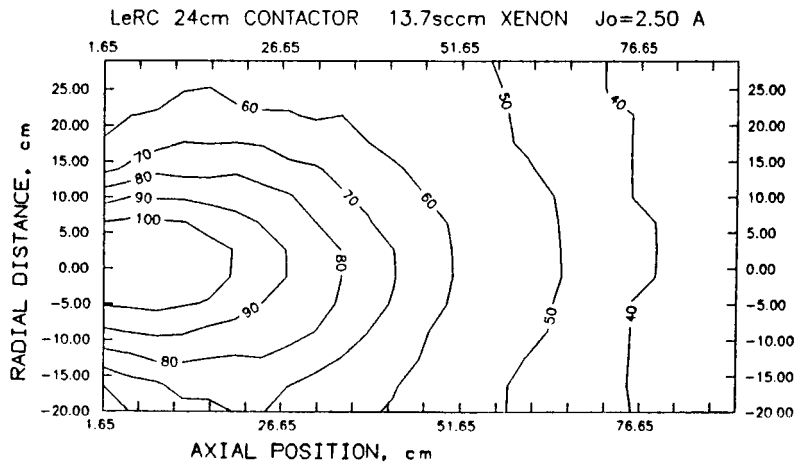


Fig. 18 Equipotential contour plot of contactor plume for 2.50 A current collection from SPS-1.

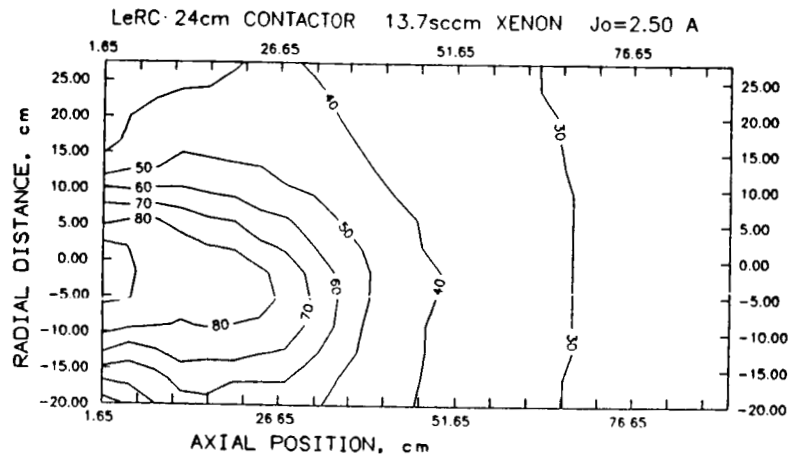


Fig. 19 Equipotential contour plot of contactor plume for 2.50 A current collection from SPS-3.

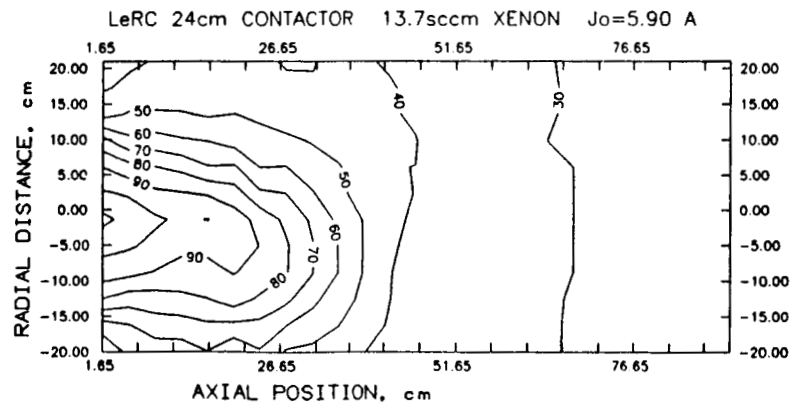


Fig. 20 Equipotential contour plot of contactor plume for 5.90 A current collection from SPS-3.



Report Documentation Page

1. Report No. NASA TM-100194		2. Government Accession No.	3. Recipient's Catalog No.	
4. Title and Subtitle Ground-Based Plasma Contactor Characterization		5. Report Date		
		6. Performing Organization Code		
7. Author(s) Michael J. Patterson and Randall S. Aadland		8. Performing Organization Report No. E-3784		
		10. Work Unit No. 906-70-25		
9. Performing Organization Name and Address National Aeronautics and Space Administration Lewis Research Center Cleveland, Ohio 44135-3191		11. Contract or Grant No.		
		13. Type of Report and Period Covered Technical Memorandum		
12. Sponsoring Agency Name and Address National Aeronautics and Space Administration Washington, D.C. 20546-0001		14. Sponsoring Agency Code		
		15. Supplementary Notes Prepared for the Second International Conference on Tethers in Space cosponsored by the ESA, AIAA, and AAS, Venice, Italy, October 6-8, 1987. Michael J. Patterson, NASA Lewis Research Center; Randall S. Aadland, University of Washington, Seattle, Washington 98105.		
16. Abstract This paper presents recent NASA Lewis Research Center (LeRC) plasma contactor experimental results, as well as a description of the plasma contractor test facility. The operation of a 24 cm diameter plasma source with hollow cathode was investigated in the "ignited-mode" regime of electron current collection from 0.1 to 7.0 A. These results are compared to those obtained with a 12 cm plasma source. Full two-dimensional plasma potential profiles were constructed from emissive probe traces of the contractor plume. The experimentally measured dimensions of the plume sheaths were then compared to those theoretically predicted using a model of a spherical double sheath. Results are consistent for currents up to approximately 1.0 A. For currents above 1.0 A, substantial deviations from theory occur. These deviations are due to sheath asphericity, and possibly volume ionization in the double-sheath region.				
17. Key Words (Suggested by Author(s)) Plasma contractor Electrodynamic tether		18. Distribution Statement Unclassified - Unlimited Subject Category 75		
19. Security Classif. (of this report) Unclassified	20. Security Classif. (of this page) Unclassified	21. No of pages 21	22. Price* A02	